Acta Crystallographica Section D
**Biological Crystallography**
ISSN 0907-4449

# Solvent behaviour in flash-cooled protein crystals at cryogenic temperatures

**M. Weik,[a]*† G. Kryger,[b] A. M. M. Schreurs,[a] B. Bouma,[a] I. Silman,[c] J. L. Sussman,[b] P. Gros[a] and J. Kroon[a]**

[a]Department of Crystal and Structural Chemistry, Bijvoet Center for Biomolecular Research, Utrecht University, Padualaan 8, 3584 CH Utrecht, The Netherlands, [b]Department of Structural Biology, Weizmann Institute of Science, Rehovot 76100, Israel, and [c]Department of Neurobiology, Weizmann Institute of Science, Rehovot 76100, Israel

† Present address: Institut de Biologie Structurale, 41 rue Jules Horowitz, F-38027 Grenoble CEDEX 1, France.

Correspondence e-mail: weik@ibs.fr

Received 21 September 2000
Accepted 16 January 2001

The solvent behaviour of flash-cooled protein crystals was studied in the range 100–180 K by X-ray diffraction. If the solvent is within large channels it crystallizes at 155 K, as identified by a sharp change in the increase of unit-cell volume upon temperature increase. In contrast, if a similar amount of solvent is confined to narrow channels and/or individual cavities it does not crystallize in the studied temperature range. It is concluded that the solvent in large channels behaves similarly to bulk water, whereas when confined to narrow channels it is mainly protein-associated. The analogy with the behaviour of pure bulk water provides circumstantial evidence that only solvent in large channels undergoes a glass transition in the 100–180 K temperature range. These studies reveal that flash-cooled protein crystals are arrested in a metastable state up to at least 155 K, thus providing an upper temperature limit for their storage and handling. The results are pertinent to the development of rational crystal annealing procedures and to the study of temperature-dependent radiation damage to proteins. Furthermore, they suggest an experimental paradigm for studying the correlation between solvent behaviour, protein dynamics and protein function.

## 1. Introduction

Flash-cooling to cryogenic temperatures is widely used to preserve macromolecular crystals during X-ray data collection (Hope, 1988; Joshua-Tor *et al.*, 1988; Garman & Schneider, 1997). Little is known in this context, however, concerning the physical state of the crystal solvent and its temperature-dependent behaviour. Studying the behaviour of solvent confined in different geometries allows detection of similarities to and differences from pure water (Mayer, 1994). Protein crystal solvent differs from pure water not only because it is confined in channels and cavities but also because of the presence of substantial concentrations of solutes such as precipitant and buffer. It is therefore beneficial to summarize briefly the behaviour of amorphous water in the temperature range utilized in the present study (for a review, see Mishima & Stanley, 1998). Although not all the peculiar properties of pure water are fully understood, it is widely accepted that amorphous solid water obtained by rapid cooling undergoes a reversible glass transition at ~130–140 K (McMillan & Los, 1965; Johari *et al.*, 1987), being transformed into a highly viscous liquid (for a general review of formation of glasses and their phenomenology, see Angell, 1995). Subsequent warming leads to crystallization into cubic ice at 150–155 K. Cubic ice transforms into ordinary hexagonal ice upon further warming above 186 K (McMillan & Los, 1965). At temperatures around the glass transition, water molecules gain rotational mobility

(Fisher & Devlin, 1995) and translational diffusion occurs prior to crystallization (Smith *et al.*, 1997). It is therefore in the 130–155 K temperature window that amorphous water exhibits liquid-like properties. Below this window diffusive motion is infinitely slow and above it is 'frozen' by the crystalline state.

In order to address the question of solvent behaviour at cryogenic temperatures, we studied protein crystals of *Torpedo californica* acetylcholinesterase (*Tc*AChE) and $\beta_2$-glycoprotein I ($\beta$2gpI) that differ in solvent content and in the manner in which the solvent is arranged in the crystal. Two crystal forms of *Tc*AChE have been studied: trigonal crystals (Sussman *et al.*, 1991; Raves *et al.*, 1997) containing 68% solvent arranged in large solvent channels and orthorhombic crystals containing 56% solvent accommodated in individual cavities and narrow channels (Raves, 1998). $\beta$2gpI crystals have an unusually high solvent content of 86% and possess even larger solvent channels than trigonal *Tc*AChE (Bouma *et al.*, 1999).

Monitoring the unit-cell parameters of flash-cooled protein crystals by X-ray diffraction as a function of temperature allowed us to show that crystal solvent in large channels crystallizes at 155 K, whereas solvent in narrow channels and individual cavities does not crystallize in the temperature range 100–180 K. The analogy with the behaviour of pure water provides circumstantial evidence that only solvent confined to large channels undergoes a glass transition in the studied temperature range.

## 2. Methods

### 2.1. Materials

Trigonal crystals of *Tc*AChE, of space group $P3_121$ and with a solvent content of 68%, were grown in 30–34%(*v*/*v*) polyethyleneglycol (PEG) 200, 0.3 *M* 2-morpholinoethanesulfonic acid (MES) pH 5.8 at 277 K (Raves *et al.*, 1997). Unit-cell parameters at 100 K are typically $a = b = 112$, $c = 137$ Å. Orthorhombic crystals of *Tc*AChE, of space group $P2_12_12_1$ and with a solvent content of 56% (Raves, 1998), were grown in 34%(*v*/*v*) PEG 200, 0.3 *M* MES pH 5.6 at 277 K. Unit-cell parameters at 100 K are typically $a = 80$, $b = 111$, $c = 163$ Å. Crystals of $\beta$2gpI of space group $C222_1$ and a solvent content of 86% were grown in 1.5 *M* $(NH_4)_2SO_4$, 2%(*v*/*v*) glycerol, 20 m*M* $CdCl_2$, 0.1 *M* HEPES pH 7.5 (Bouma *et al.*, 1999). Unit-cell parameters at 100 K are typically $a = 161$, $b = 165$, $c = 115$ Å.

### 2.2. Data collection and processing

*Tc*AChE crystals were transferred for ~1 min into a drop of mineral oil before being mounted in a cryoloop. $\beta$2gpI crystals were equilibrated for about 20 s at 277 K in 1.65 *M* $(NH_4)_2SO_4$, 35%(*v*/*v*) glycerol, 20 m*M* HEPES pH 7.5 before being similarly mounted. Crystals were subsequently flash-cooled at 100–105 K in an $N_2$ cold-gas-stream device (Oxford Cryosystems, Oxford, England) which was used to control the temperature during heating and cooling. X-ray measurements were carried out on a Nonius $\kappa$-CCD diffractometer mounted on a sealed-tube source. Cu $K\alpha$ ($\lambda = 1.54$ Å) radiation was used in all experiments on protein crystals, whereas Mo $K\alpha$ ($\lambda = 0.71$ Å) radiation was used for reference experiments with solvent only.

The crystals were warmed from 100 or 105 to 180 K and recooled to the starting temperature in 5 K steps (with a heating and cooling rate of 360 K $h^{-1}$) according to two different experimental protocols on two different time scales. Using the first protocol ('type I' experiment, *i.e.* on a long time scale), five consecutive data sets for unit-cell determination were collected at each temperature. Each data set was recorded over about 24 min. Thus, the crystal spent 120 min at a constant temperature between two temperature steps. This type of experiment was carried out on both *Tc*AChE crystal forms and on $\beta$2gpI crystals. Control experiments utilizing the same experimental protocol were performed on the cryoprotective solutions used for *Tc*AChE and $\beta$2gpI, *i.e.* 34%(*v*/*v*) PEG 200, 0.3 *M* MES pH 5.8 and 1.65 *M* $(NH_4)_2SO_4$, 35%(*v*/*v*) glycerol, 20 m*M* HEPES pH 7.5, respectively. For this purpose, a thin film of the cryoprotective solution in a similarly sized cryoloop was flash-cooled at 100 K.

Using the second protocol, only one data set was collected at each temperature ('type II' experiment, *i.e.* on a short time scale). Collection of a data set took ~19 min for trigonal *Tc*AChE crystals, while it took only about 11 min for $\beta$2gpI crystals. Each data set in both types of experiment was collected with a $\varphi$ rotation of 1°.

Before initiation of the warming and cooling protocol in both types of experiment, a single data set was collected with a total exposure time of 20 min from each flash-cooled crystal in order to determine accurate unit-cell parameters by applying the $\varphi$–$\chi$ method ($\varphi = 1$, $\chi = 5°$; Duisenberg *et al.*, 2000) at four different $\varphi$ positions 90° apart, so as to provide data as input for the autoindexing program *DirAx* (Duisenberg, 1992). The resulting orientation matrix was then continuously refined using *DENZO* (Otwinowski & Minor, 1997) against the data collected at the different temperatures during the warming and cooling procedure.

In order to monitor ice formation in the crystal, intensities in the diffraction pattern were radially integrated and were summed in the 4.23–3.19 Å resolution shell.

## 3. Results

Results of the 'type I' experiments are shown in Fig. 1, *i.e.* the relative unit-cell volume, the integrated ice-ring intensities and the temperature of flash-cooled orthorhombic (Fig. 1*a*) and trigonal (Fig. 1*b*) *Tc*AChE and $\beta$2gpI (Fig. 1*c*) crystals as a function of the elapsed experimental time upon warming from 105 to 180 K. At ~155 K (indicated by the vertical line across Fig. 1), a sharp increase in unit-cell volume was observed for the trigonal *Tc*AChE (Fig. 1*b*) and the $\beta$2gpI crystals (Fig. 1*c*) but not for the orthorhombic *Tc*AChE crystals (Fig. 1*a*). For all three crystals, below 155 K the unit-cell volume increased slightly as the temperature was raised but remained relatively constant at constant temperature; no ice-ring formation was observed (Figs. 1*a*–1*c*). At temperatures above 155 K, the unit-

cell volumes of the trigonal *Tc*AChE crystal (Fig. 1*b*) and the $\beta$2gpI crystal (Fig. 1*c*) showed altered behaviour, increasing even at constant temperature. At 180 K, the relative unit-cell volume increase relative to the volume at 105 K was 1.2 $\pm$ 0.1% (unit-cell parameters *a*, *b* and *c* increased by 0.23, 0.39 and 0.51%, respectively), 3.7 $\pm$ 0.1% (*a*, 1.45; *c*, 0.80%) and 7.5 $\pm$ 0.3% (*a*, 0.84; *b*, 4.84; *c*, 1.69%) for the orthorhombic and trigonal *Tc*AChE crystals and the $\beta$2gpI crystals, respectively. A clear onset of ice formation at 155 K was seen in all three crystals (Figs. 1*a*–1*c*). Inspection of the diffraction patterns before summation in the 4.23–3.19 Å resolution shell revealed that it was the cubic ice form that crystallizes at 155 K. At 175–180 K, diffraction peaks characteristic of hexagonal ice also started to appear in the diffraction pattern. Control experiments with only the mother liquor of trigonal and orthorhombic *Tc*AChE crystals in the loop also showed clear ice formation at 155 K (data not shown). In contrast, the cryoprotective solution (containing 35% glycerol) used for $\beta$2gpI crystals crystallized at 170–175 K (data not shown). Attempts to vitrify the mother liquor (containing only 2% glycerol) of $\beta$2gpI crystals by flash-cooling failed, as judged by the presence of Bragg peaks of crystalline ice in the diffraction pattern at 100 K.

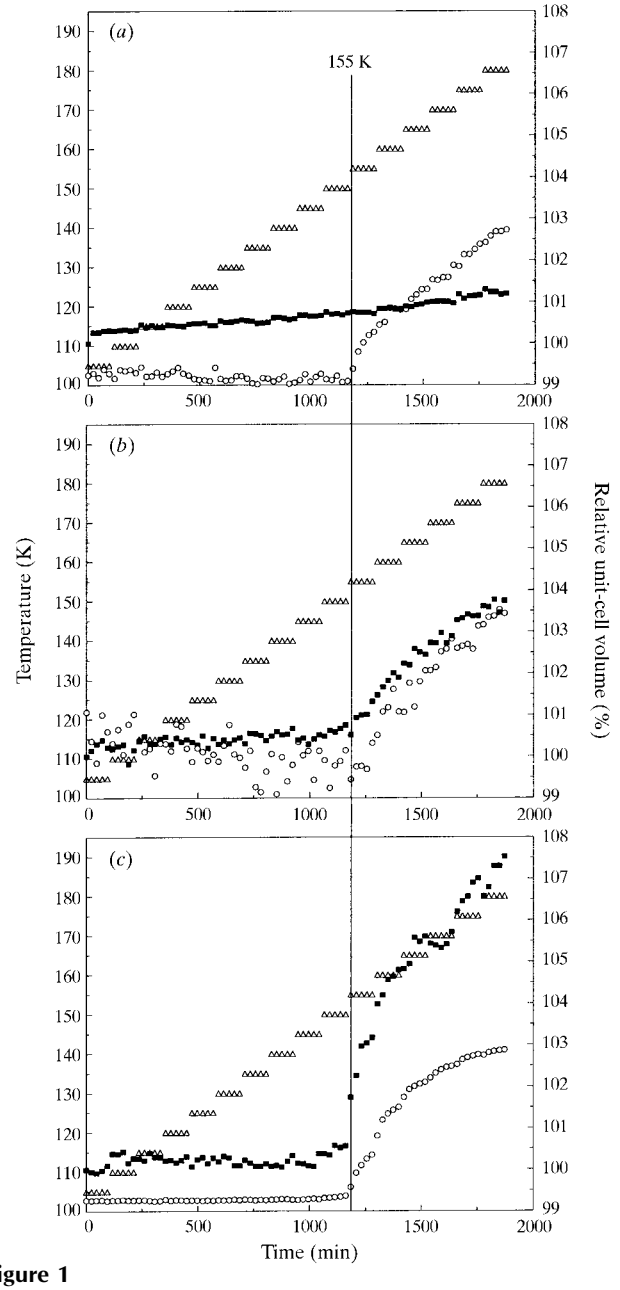


**Figure 1**
Relative unit-cell volume (closed squares), ice intensity (open circles) and temperature (open triangles) as a function of elapsed experimental time for (*a*) orthorhombic and (*b*) trigonal *Tc*AChE crystals and (*c*) $\beta$2gpI crystals for 'type I' experiments. Unit-cell volumes are normalized to the value at 105 K. Ice-ring intensities were determined by radially integrating and, in the 4.23–3.19 Å resolution shell, summing the intensities of the most prominent ice rings. Ice intensities do not refer to either of the *y* axes and are on an arbitrary scale, but were zero at 105 K. Each time point corresponds to one data set (~24 min per data set). Five data sets were collected at each constant temperature between temperature steps.

A different pattern of behaviour was observed in the 'type II' experiments in which the experimental time frame was reduced approximately sixfold for trigonal *Tc*AChE crystals (Fig. 2*a*) and approximately tenfold for $\beta$2gpI crystals (Fig. 2*b*). On this experimental time scale at 155 K the trigonal *Tc*AChE crystal (Fig. 2*a*) showed neither an abrupt increase in unit-cell volume nor ice formation. The relative volume increase at 180 K was 0.85 $\pm$ 0.1% (*a*, 0.28; *c*, 0.25%) with respect to 100 K. The $\beta$2gpI crystal (Fig. 2*b*) showed a similar unit-cell volume increase at 180 K, 7.4 $\pm$ 0.3% (*a*, 2.48%; *b*, 3.80%; *c*, 0.94%), and ice formation as in the experiment on a longer time scale (*i.e.* 7.5%; Fig. 1*c*).

Fig. 3 shows the changes in unit-cell volume of trigonal *Tc*AChE crystals upon recooling from 180 K back to 100 and 105 K on the two different time scales. Unit-cell parameter changes were irreversible on the long (Fig. 3*a*) time scale and reversible on the short (Fig. 3*b*) time scale. In the experiment on the short time scale the unit-cell volume even fell below its starting value (Fig. 3*b*). Note that the scale of Fig. 3(*b*) is altered compared with Fig. 2(*a*). This allows visualization of the fine structure in unit-cell volume changes, *i.e.* that the unit-cell volume remained virtually constant between 130 and 155 K both upon warming and recooling on a short experimental time scale. Fig. 3(*b*) shows the results of experiments performed on two different crystals according to identical schemes in order to investigate the reproducibility of the characteristic unit-cell volume changes. Unit-cell volume changes of the $\beta$2gpI crystals were irreversible even in the short time-scale experiments (data not shown). All the experiments presented have been repeated at least twice with different crystals of similar size and the results showed that the observed effects are crystal independent.

X-ray data quality, as monitored by the number of observed reflections, remained constant over the entire studied temperature range in all experiments in which no sharp increase in unit-cell volume was observed (*i.e.* those reported in Figs. 1*a*, 2*a* and 3*b*). However, this number decreased drastically at 155 K in experiments in which a sharp increase in unit-cell volume was observed (*i.e.* those reported in Figs. 1*b*, 1*c*, 2*b* and 3*a*). Owing to the limited $\varphi$ range used in the

present study, however, we could not obtain accurate information on the high-resolution limit of diffraction and the mosaicity of the crystal during the course of the experiments.

## 4. Discussion

The aim of the present study was to assess solvent behaviour in flash-cooled protein crystals in the temperature range 100–180 K. Protein crystals were chosen that differ both in solvent content and in the way in which the solvent is arranged within the crystal. Orthorhombic and trigonal *Tc*AChE crystals have similar solvent contents (56 and 68%, respectively), yet the arrangement of solvent is different. In the orthorhombic crystals, the solvent is arranged in cavities and narrow channels of ∼10 Å in their smallest dimension (Raves, 1998; Fig. 4*a*), whereas in the trigonal *Tc*AChE crystals the solvent is located predominantly in large channels ∼65 Å in diameter that run straight through the crystal (Fig. 4*b*). $\beta$2gpI crystals have an unusually high solvent content of 86% and large solvent channels along each cell axis, the largest of which is aligned with the *c* axis and has an extent of ∼80 Å in its smallest dimension (Fig. 4*c*).

Unit-cell expansion upon increasing the temperature allowed us to gain insight into the crystal solvent behaviour. In experiments on an identical time scale, only the crystals with large solvent channels, *i.e.* trigonal *Tc*AChE (Fig. 1*b*) and $\beta$2gpI (Fig. 1*c*), showed a sharp increase in unit-cell volume at ∼155 K. The formation of ice rings in the diffraction pattern was observed at the same temperature. We conclude that the sharp change in unit-cell volume at 155 K is a consequence of crystallization of the solvent within the channels of the crystal. In contrast, the orthorhombic *Tc*AChE crystals (narrow solvent channels) did not show a sharp increase in unit-cell volume anywhere in the 100–180 K temperature range (Fig. 1*a*), indicating that the solvent *within* these crystals did not crystallize. The fact that ice rings in the diffraction pattern appeared nevertheless above 155 K is attributed to the crystallization of a thin solvent layer located between the crystal

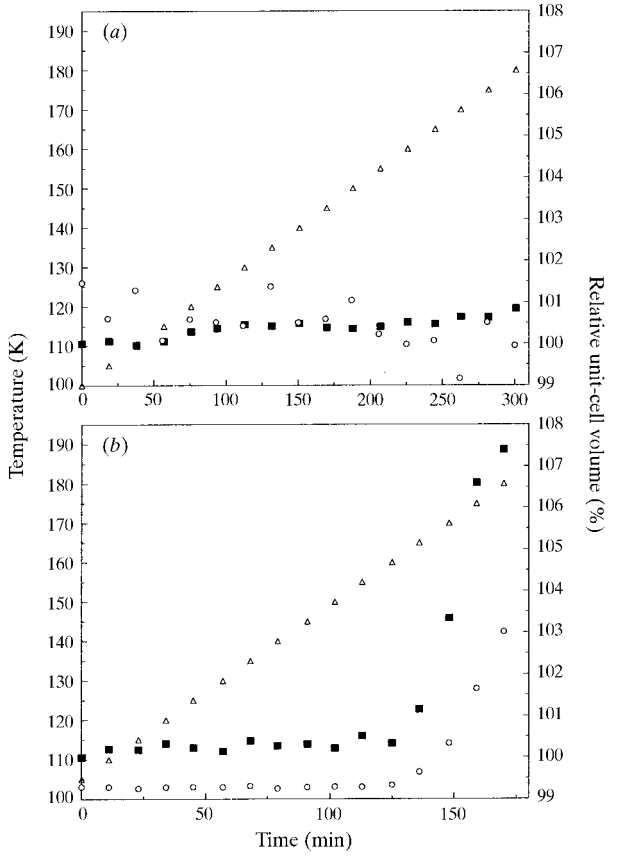


**Figure 2**
Relative unit-cell volume (closed squares), ice intensity (open circles) and temperature (open triangles) as a function of elapsed experimental time for (*a*) trigonal *Tc*AChE crystals and (*b*) $\beta$2gpI crystals for 'type II' experiments. Unit-cell volumes were normalized to the value at 100 and 105 K, respectively. Ice-ring intensities were determined as in Fig. 1. Ice intensities do not refer to either of the *y* axes and are on an arbitrary scale, but were zero at 100 and 105 K, respectively. Each time point corresponds to one data set [∼19 min per data set in (*a*) and ∼11 min per data set in (*b*)]. In contrast to Fig. 1, only one data set was collected at each constant temperature between two temperature steps.

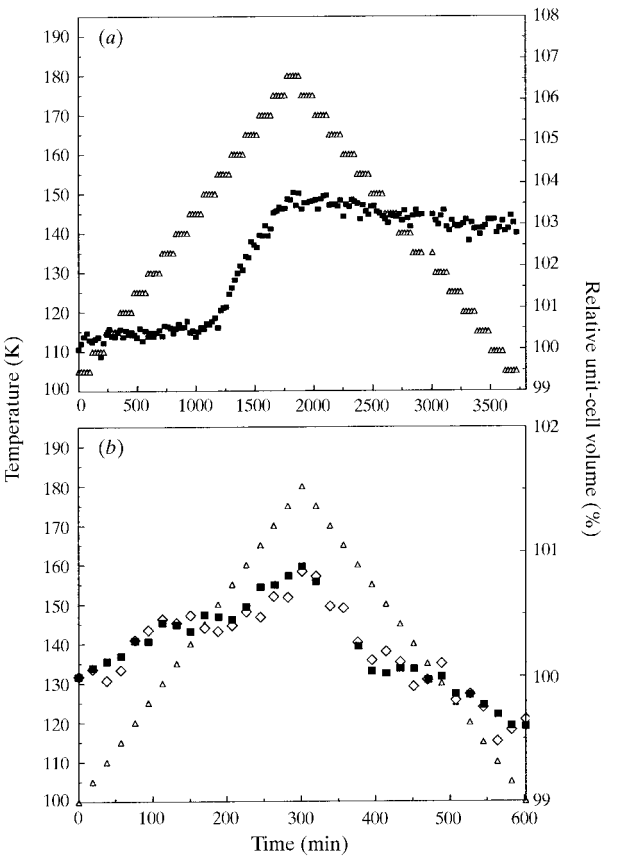


**Figure 3**
Relative unit-cell volumes (closed squares and open diamonds) and temperature (open triangles) as a function of elapsed experimental time for trigonal *Tc*AChE. Each time point corresponds to one data set. Five and one data sets were collected at each constant temperature between two temperature steps in (*a*) and (*b*), respectively. Data corresponding to the heating process, which are represented as closed squares in (*a*) and as open diamonds in (*b*), are identical to the data shown in Figs. 1(*b*) and 2(*a*), respectively. Data represented by closed squares and open diamonds in (*b*) were collected on two different crystals according to the same experimental procedure.

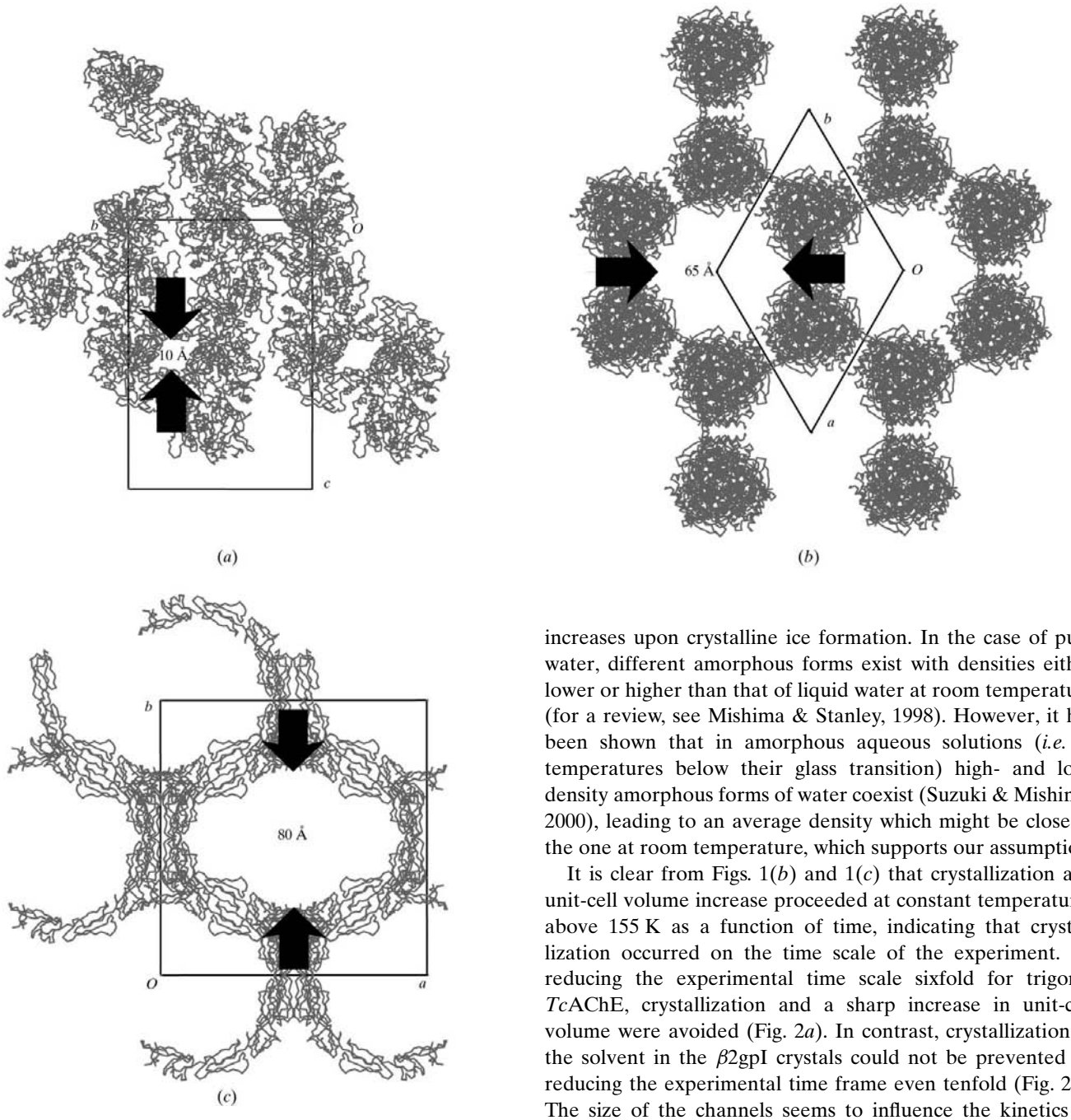


**Figure 4**
Packing diagram for (*a*) orthorhombic *Tc*AChE viewed down the *a* axis, (*b*) for trigonal *Tc*AChE viewed down the *c* axis and (*c*) for $\beta$2gpI viewed down the *c* axis. The proteins are shown with a $C^{\alpha}$ trace. Figs. 4(*a*) and 4(*b*) are taken from Raves (1998).

and the protective mineral oil. If the ice rings had been a consequence of crystallization of the solvent within the crystal, we would have expected the increase in unit-cell volume to show a non-linear behaviour similar to that observed for trigonal *Tc*AChE and $\beta$2gpI.

Implicit in our reasoning is the assumption that the crystal solvent in its amorphous form has a density similar to that in the liquid state at room temperature, *i.e.* that its volume increases upon crystalline ice formation. In the case of pure water, different amorphous forms exist with densities either lower or higher than that of liquid water at room temperature (for a review, see Mishima & Stanley, 1998). However, it has been shown that in amorphous aqueous solutions (*i.e.* at temperatures below their glass transition) high- and low-density amorphous forms of water coexist (Suzuki & Mishima, 2000), leading to an average density which might be close to the one at room temperature, which supports our assumption.

It is clear from Figs. 1(*b*) and 1(*c*) that crystallization and unit-cell volume increase proceeded at constant temperatures above 155 K as a function of time, indicating that crystallization occurred on the time scale of the experiment. By reducing the experimental time scale sixfold for trigonal *Tc*AChE, crystallization and a sharp increase in unit-cell volume were avoided (Fig. 2*a*). In contrast, crystallization of the solvent in the $\beta$2gpI crystals could not be prevented by reducing the experimental time frame even tenfold (Fig. 2*b*). The size of the channels seems to influence the kinetics of crystallization of solvent – the larger the channel, the quicker the crystallization process. However, we cannot exclude the possibility that the difference in cryoprotective solutions was partially or entirely responsible for the observed difference in crystallization kinetics. If a flash-cooled trigonal *Tc*AChE crystal is held for 15 h at 155 K the unit-cell volume remains constant. If the temperature is raised further and held at 160 K, both a progressive increase in unit-cell volume and ice formation are observed (data not shown). Even after 48 h at 160 K, unit-cell volume increase (which reached 1.6% with respect to 100 K) and ice formation continued to progress.

The question of whether the observed unit-cell volume changes are reversible was addressed by cooling trigonal *Tc*AChE and $\beta$2gpI crystals stepwise after the heating process.

Unit-cell volume changes were irreversible when they arose from crystallization of the crystal solvent (Fig. 3*a*). In contrast, the unit-cell volume changes observed in the absence of crystallization were fully reversible (Fig. 3*b*), indicating that they were a consequence of thermal expansion of the solvent and/or the protein molecules.

Frauenfelder *et al.* (1987) estimated the linear thermal expansion coefficient for myoglobin molecules to be $115 \times 10^{-6}$ K$^{-1}$. Assuming a similar coefficient for *Tc*AChE and for $\beta$2gpI would indicate that 0.9% of the unit-cell volume increase upon raising the temperature from 100 to 180 K can be attributed to the thermal expansion of the protein molecules alone. Comparing this value with the measured unit-cell volume increase of orthorhombic *Tc*AChE (1.2%; Fig. 1*a*) and of trigonal *Tc*AChE on the reduced experimental time scale (0.85%; Figs. 2*a* and 3*b*) indicates that the unit-cell volume increase is dominated by expansion of the protein molecules if the crystal solvent remains in the amorphous phase rather than crystallizing. However, if crystallization does occur (Figs. 1*b*, 1*c*, 2*b* and 3*a*), the unit-cell volume increase is dominated by the difference in volume between the amorphous and the crystalline form of the solvent. We note that the observed volume increase of 7.5% between 105 and 180 K for $\beta$2gpI crystals would correspond to the increase in volume if the crystal solvent were composed of pure amorphous solid water with a density identical to that of liquid water at room temperature which crystallizes fully to cubic (or hexagonal) ice.

The observed volume expansion in the trigonal *Tc*AChE crystals in the 'type I' experiment is anisotropic. The cell axis along the solvent channel (*c* axis) shows about half of the relative expansion of the other cell axes (*a* and *b* axes). In this direction, the solvent can expand during crystallization without displacing protein molecules.

Our observation that the solvent in trigonal *Tc*AChE and $\beta$2gpI crystals crystallizes at 155 K indicates that solvent in large channels behaves similarly to bulk water, in contrast to solvent in narrow channels. This provides circumstantial evidence but does not prove that only solvent in large channels undergoes a glass transition in the 100–180 K temperature range, *i.e.* prior to crystallization at 155 K. It is interesting to note that the unit-cell volume of trigonal *Tc*AChE remains constant in the 130–155 K temperature window, both upon warming and recooling, if crystallization is avoided by a reduced experimental time frame (Fig. 3*b*). This coincides with the temperature window in which pure bulk water has liquid-like properties (Mishima & Stanley, 1998) and leads us to speculate that the crystal solvent may have similar liquid-like properties in that temperature window.

It is interesting to note that in the control experiment, in the absence of protein crystals, the cryoprotective solution (containing 35% glycerol) used for $\beta$2gpI crystals crystallizes at 170–175 K, *i.e.* 20 K higher than the solvent within the $\beta$2gpI crystals. It has been reported that the glass-transition temperature and hence the crystallization temperature of a glycerol–water binary mixture increases with increasing glycerol concentration (Harran, 1978). We conclude, therefore, that the solvent within the channels of the $\beta$2gpI crystals, after the short soaking procedure of 20 s in the cryoprotective solution, still contains a glycerol concentration close to that of the mother liquor (2%). This suggests that the glass-transition temperature of solvent confined in large channels might be shifted to higher temperatures by adding glycerol, provided that this does not affect the stability of the protein crystal.

Protein surfaces are covered by a monolayer of highly ordered water molecules (the hydration shell) which behaves differently from bulk water and which is non-freezable (see Rupley & Careri, 1991 and references therein). Furthermore, some order in the water out to 4.5–8 Å from the protein surface has been reported depending on the protein system studied (Rupley & Careri, 1991; Jiang & Brünger, 1994). The solvent in channels as narrow as 10 Å thus contains water which is either directly associated with or influenced by the protein surface and which therefore differs from solvent water in large channels and from pure water. This is indeed in line with our observations.

The question arises as to how far radiation damage might contribute to the observed volume increase. It has been observed that exposure of protein crystals to synchrotron radiation causes specific structural and chemical damage to the protein (Weik *et al.*, 2000; Ravelli & McSweeney, 2000; Burmeister, 2000) as well as an increase in unit-cell volume (Yonath *et al.*, 1998; Ravelli & McSweeney, 2000; Burmeister, 2000). A linear dependency of the unit-cell volume increase on the absorbed dose has been suggested (Ravelli & McSweeney, 2000; Burmeister, 2000). A total absorbed dose of about $10^7$ Gy at a constant temperature of 100 K led to a relative unit-cell volume increase of 0.11% for trigonal *Tc*AChE (Ravelli & McSweeney, 2000). We calculated the total absorbed dose to be in the order of $10^4$ Gy for the extended experiment on trigonal *Tc*AChE (Fig. 1*b*), which would give rise to a unit-cell volume increase of 0.0001% if the linear dependency determined at 100 K were valid over the entire 100–180 K temperature range. This value is negligible when compared with the observed unit-cell volume increase of 3.7% (Fig. 1*b*). However, at equal absorbed doses, we expect the unit-cell volume increase arising from radiation damage to be different at temperatures above the glass transition to that at 100 K. This would be because of increased mobility of radicals created by X-ray irradiation at temperatures above the presumed glass transition owing to the decreased solvent viscosity. In any case, our conclusion concerning the difference in behaviour of crystal solvent in large and in narrow channels is independent of the influence of radiation damage.

Spatial fluctuation of unit-cell parameters is perhaps the main imperfection in flash-cooled protein crystals giving rise to high mosaicity (Nave, 1998). Increasing the solvent mobility by raising the temperature above the solvent glass transition might induce a relaxation process which would narrow the distribution of unit-cell parameters. Such an approach could be useful in developing rational crystal-annealing protocols aimed at improving crystal order, similar to the empirical procedures that have been reported (Yeh & Hol, 1998; Harp *et al.*, 1998, 1999), but without the necessity of warming the

crystal to room temperature. Annealing of flash-cooled protein crystals at temperatures just below 155 K might lead to densification of the solvent owing to enthalpy relaxation – a process commonly observed in amorphous solids (Johari *et al.*, 1991). Densification of the solvent upon annealing might also explain our observation that the unit-cell volume drops below its initial value upon temperature cycling from 105 to 180 K and back to 105 K on a time scale that prevents ice formation (Fig. 3*b*).

Our studies reveal that flash-cooled protein crystals are arrested in a metastable state up to at least 155 K without crystallization of the solvent. Thus, our results provide a high-temperature limit for the storage and handling of flash-cooled protein crystals. This might be of importance for the design of experiments in which minimization of required cooling power is important, such as diffraction experiments in space (E. Garman, personal communication).

The study of solvent behaviour in flash-cooled protein crystals is also of relevance to the current discussion concerning the dynamic correlation between proteins and their surrounding solvent (Vitkup *et al.*, 2000, Réat *et al.*, 2000). A dynamic transition in protein molecules can be essential for biological function, as has been shown for myoglobin (Doster *et al.*, 1989), bacteriorhodopsin (Ferrand *et al.*, 1993; Réat *et al.*, 1998) and ribonuclease A (Rasmussen *et al.*, 1992). A cross-correlation between the dynamic behaviour of proteins and the surrounding solvent has been proposed (Doster *et al.*, 1986; Frauenfelder & Gratton, 1986). Indeed, it has been reported that myoglobin embedded in trehalose glasses does not undergo a dynamic transition (Cordone *et al.*, 1999), whereas such a transition does take place in hydrated myoglobin at 180 K (Doster *et al.*, 1989). It will be interesting to investigate the dynamic behaviour of *Tc*AChE in both the trigonal and the orthorhombic crystal form. Temperature-controlled protein crystallography (Ringe & Petsko, 1985; Tilton *et al.*, 1992) is a valuable tool that might show whether the crystal solvent glass transition directly triggers a dynamic transition in the protein molecules and whether the absence of a solvent glass transition abolishes such a dynamic transition. In particular, use of caged substrates (Peng & Goeldner, 1998) in temperature-controlled crystallographic experiments on *Tc*AChE may permit a study of the correlation between solvent behaviour, protein dynamics and protein function.

We thank Giuseppe Zaccai and Elspeth Garman for fruitful discussions and critical and constructive reading of the manuscript. MW thanks the European Molecular Biology Organization for a long-term fellowship during part of the course of this work. IS is Bernstein–Mason Professor of Neurochemistry. This work was supported by the US Army Medical and Material Command under contract number DAMD17-97-2-7022, the EU 4th Framework Program in Biotechnology, the Kimmelman Center for Biomolecular Structure and Assembly (Rehovot, Israel) and the Dana Foundation.

## References

Angell, C. A. (1995). *Science*, **267**, 1924–1935.
Bouma, B., de Groot, P. G., van den Elsen, J. M. H., Ravelli, R. B. G., Schouten, A., Simmelink, M. J. A., Derksen, R. H. W. M., Kroon, J. & Gros, P. (1999). *EMBO J.* **18**, 5166–5174.
Burmeister, W. P. (2000). *Acta Cryst.* D**56**, 328–341.
Cordone, L., Ferrand, M., Vitrano, E. & Zaccai, G. (1999). *Biophys. J.* **76**, 1043–1047.
Doster, W., Bachleitner, A., Dunau, R., Hiebl, M. & Lüscher, E. (1986). *Biophys. J.* **50**, 213–219.
Doster, W., Cusack, S. & Petry, W. (1989). *Nature (London)*, **337**, 754–756.
Duisenberg, A. J. M. (1992). *J. Appl. Cryst.* **25**, 92–96.
Duisenberg, A. J. M., Hooft, R. W. W., Schreurs, A. M. M. & Kroon, J. (2000). *J. Appl. Cryst.* **33**, 893–898.
Ferrand, M., Dianoux, A. J., Petry, W. & Zaccai, G. (1993). *Proc. Natl Acad. Sci. USA*, **90**, 9668–9672.
Fisher, M. & Devlin, J. P. (1995). *J. Phys. Chem.* **99**, 11584–11590.
Frauenfelder, H. & Gratton, E. (1986). *Methods Enzymol.* **127**, 207–216.
Frauenfelder, H., Hartmann, H., Karplus, M., Kuntz, I. D., Kuriyan, J., Parak, F., Petsko, G. A., Ringe, D., Tilton, R. F., Connolly, M. L. & Max, N. (1987). *Biochemistry*, **26**, 254–261.
Garman, E. F. & Schneider, T. R. (1997). *J. Appl. Cryst.* **30**, 211–237.
Harp, J. M., Hanson, B. L., Timm, D. E. & Bunick, G. J. (1999). *Acta Cryst.* D**55**, 1329–1334.
Harp, J. M., Timm, D. E. & Bunick, G. J. (1998). *Acta Cryst.* D**54**, 622–628.
Harran, D. (1978). *Bull. Soc. Chim. Fr.*, pp. 40–44.
Hope, H. (1988). *Acta Cryst.* B**44**, 22–26.
Jiang, J.-S. & Brünger, A. T. (1994). *J. Mol. Biol.* **243**, 100–115.
Johari, G. P., Hallbrucker, A. & Mayer, E. (1987). *Nature (London)*, **330**, 552–553.
Johari, G. P., Hallbrucker, A. & Mayer, E. (1991). *J. Chem. Phys.* **95**, 2955–2964.
Joshua-Tor, L., Rabinovich, D., Hope, H., Frolow, F., Appella, E. & Sussman, J. L. (1988). *Nature (London)*, **334**, 82–84.
McMillan, J. A. & Los, S. C. (1965). *Nature (London)*, **206**, 806–807.
Mayer, E. (1994). *Hydrogen Bonded Networks*, edited by M.-C. Bellissent-Funel & J. C. Dore, pp. 355–372. Dordrecht: Kluwer Academic Publishers.
Mishima, A. & Stanley, H. E. (1998). *Nature (London)*, **396**, 329–335.
Nave, C. (1998). *Acta Cryst.* D**54**, 848–853.
Otwinowski, Z. & Minor, W. (1997). *Methods Enzymol.* **276**, 307–326.
Peng, L. & Goeldner, M. (1998). *Methods Enzymol.* **291**, 265–278.
Rasmussen, B. F., Stock, A. M., Ringe, D. & Petsko, G. A. (1992). *Nature (London)*, **357**, 423–424.
Ravelli, R. B. & McSweeney, S. M. (2000). *Structure Fold. Des.* **8**, 315–328.
Raves, M. L. (1998). PhD thesis, Weizmann Institute of Science, Israel.
Raves, M. L., Harel, M., Pang, Y.-P., Silman, I., Kozikowski, A. P. & Sussman, J. L. (1997). *Nature Struct. Biol.* **4**, 57–63.
Réat, V., Dunn, R., Ferrand, M., Finney, J. L., Daniel, R. M. & Smith, J. C. (2000). *Proc. Natl Acad. Sci. USA*, **97**, 9961–9966.
Réat, V., Patzelt, H., Ferrand, M., Pfister, C., Oesterhelt, D. & Zaccai, G. (1998). *Proc. Natl Acad. Sci. USA*, **95**, 4970–4975.
Ringe, D. & Petsko, G. A. (1985). *Prog. Biophys. Mol. Biol.* **45**, 197–235.
Rupley, J. A. & Careri, G. (1991). *Adv. Protein Chem.* **41**, 37–172.
Smith, R. S., Huang, C. & Kay, B. D. (1997). *J. Phys. Chem. B*, **101**, 6123–6126.
Sussman, J. L., Harel, M., Frolow, F., Oefner, C., Goldman, A., Toker, L. & Silman, I. (1991). *Science*, **253**, 872–879.
Suzuki, Y. & Mishima, O. (2000). *Phys. Rev. Lett.* **85**, 1322–1325.

Tilton, R. F. Jr, Dewan, J. C. & Petsko, G. A. (1992). *Biochemistry*, **31**, 2469–2481.
Vitkup, D., Ringe, D., Petsko, G. A. & Karplus, M. (2000). *Nature Struct. Biol.* **7**, 34–38.
Weik, M., Ravelli, R. B., Kryger, G., McSweeney, S., Raves, M. L., Harel, M., Gros, P., Silman, I., Kroon, J. & Sussman, J. L. (2000). *Proc. Natl Acad. Sci. USA*, **97**, 623–628.
Yeh, J. I. & Hol, W. G. J. (1998). *Acta Cryst.* D**54**, 479–480.
Yonath, A., Harms, J., Hansen, H. A., Bashan, A., Schlunzen, F., Levin, I., Koelln, I., Tocilj, A., Agmon, I., Peretz, M., Bartels, H., Bennett, W. S., Krumbholz, S., Janell, D., Weinstein, S., Auerbach, T., Avila, H., Piolleti, M., Morlang, S. & Franceschi, F. (1998). *Acta Cryst.* A**54**, 945–955.